universe

MDPI

Article

Analysis of the Capability of Detection of Extensive Air Showers by Simple Scintillator Detectors

Jerzy Seweryn Pryga [1,*], Weronika Stanek [2], Krzysztof Wiesław Woźniak [3], Piotr Homola [3], Kevin Almeida Cheminant [3], Sławomir Stuglik [3], David Alvarez-Castillo [3], Łukasz Bibrzycki [4], Marcin Piekarczyk [4], Olaf Bar [4], Tadeusz Wibig [5], Arman Tursunov [6] and Michał Niedźwiecki [7], Tomasz Sośnicki [8] and Krzysztof Rzecki [8]

1 Faculty of Physics, Astronomy and Applied Computer Science, Jagiellonian University in Cracow, Gołębia 24, 31-007 Cracow, Poland
2 Faculty of Physics and Applied Computer Science, AGH University of Science and Technology, 30 Mickiewicza Ave., 30-059 Cracow, Poland
3 Institute of Nuclear Physics Polish Academy of Sciences, Walerego Eljasza Radzikowskiego 152, 31-342 Cracow, Poland
4 Faculty of Exact and Natural Sciences, Pedagogical University of Cracow, Podchorążych 2, 30-084 Cracow, Poland
5 Faculty of Physics and Applied Informatics, University of Lodz, Pomorska 149/153, 90-236 Lodz, Poland
6 Institute of Physics, Silesian University in Opava, Bezručovo nám 13, CZ-74601 Opava, Czech Republic
7 Department of Computer Science, Cracow University of Technology, ul. Warszawska 24, 31-155 Cracow, Poland
8 Faculty of Electrical Engineering, Automatics, Computer Science and Biomedical Engineering, AGH University of Science and Technology, 30 Mickiewicza Ave., 30-059 Cracow, Poland
* Correspondence: jerzy.pryga@student.uj.edu.pl

Citation: Pryga, J.S.; Stanek, W.; Woźniak, K.W.; Homola, P.; Almeida Cheminant, K.; Stuglik, S.; Alvarez-Castillo, D.; Bibrzycki, Ł.; Piekarczyk, M.; Bar, O.; et al. Analysis of the Capability of Detection of Extensive Air Showers by Simple Scintillator Detectors. *Universe* **2022**, *8*, 425. https://doi.org/10.3390/universe8080425

Academic Editor: Maria Vasileiou

Received: 13 May 2022
Accepted: 8 August 2022
Published: 18 August 2022

Abstract: One of the main objectives of the CREDO project is to register cosmic-ray cascades in many distributed detectors in the search for so-called Cosmic-Ray Ensembles (CRE). This requires precise knowledge of the probability of detection of individual Extensive Air Showers (EAS) in a very wide range of energies and an analysis of their correlations. The standard approach based on detailed and extensive simulations is not possible for many such systems; thus, a faster method is developed. Knowing the characteristics of EAS from more general simulations, any required probability is calculated. Such probability depends on particle density at a given point, which is a function of the distance from the centre of the cascade, the energy, mass and the zenith angle of the primary cosmic-ray particle. It is necessary to use proper distribution of the number of secondary particles reaching the ground and their fluctuations. Finally, to calculate the total probability of EAS detection, the primary cosmic-ray spectrum and abundance of various particles in it have to be taken into account. The effective probability can be used to estimate the expected number of EAS events measured by a set of small detectors. In this work, results from several versions of calculations, with different complexity levels, are presented and compared with the first measurement performed with a test detector system. These results confirm that the majority of events observed with this small detector array are caused by cosmic-ray particles with very high energies. Such analysis can be also useful for the design of more effective systems in the future. Slightly larger systems of simple detectors may be used to distinguish cascades initiated by photons from those started from other primary cosmic-ray particles.

Keywords: extensive air showers; detector; cascade; events; coincidence; signal; correlations; CORSIKA simulations; CREDO collaboration; cosmic rays

1. Introduction

The main purpose of Cosmic Ray Extremely Distributed Observatory (CREDO) [1] is the search of Cosmic-Ray Ensembles (CRE)—groups of energetic cosmic rays correlated in time and space. They may appear if some number of high energy cosmic-ray particles of a

common origin enter the Earth's atmosphere at approximately the same time. Occurrences of correlated in time multiple Extended Air Showers (EAS) were reported in the past [2,3], but they are only hints of unusual events. One of the sources of CRE may be ultra-high energy photons, which, according to some models, can be generated within the Solar system [4]. The main motivation for this work is to provide information about capabilities of one of the methods of detection of EAS proposed for the CREDO project whose goal requires monitoring of cosmic rays and EAS on a global scale with the use of detectors, which can be used not only in laboratories by scientists but also in schools or outdoors by students and amateurs. It is a part of a long-range plan of creating a global network of cosmic-ray detectors for CREDO. This intended use enforces many limitations on considered detector arrays like low price, simple construction and thus easy installation, the necessity of being able to send data to a server, low energy consumption, and reliability. For now, the main source of data for this task is a mobile phone application called a CREDO Detector, which uses the smartphone camera as a detector [5]. One of the other proposed ideas is analysed in this work: several scintillator detectors connected in a coincidence system. When several devices give the signal at almost the same time, it may indicate an occurrence of a cosmic-ray cascade. Several different prototypes of such devices have already been constructed and tested with promising results [6,7]. To be confident that the registered signals are due to cosmic-ray showers, an analysis for each detector array like the one presented in this work is necessary. It is especially necessary to determine if, in a simple system, the frequency of events caused by background particles is sufficiently lower than those caused by EAS. The study presented in this work tries to provide tools to estimate if an analysed type of detector array can be reliable and efficient enough to be used successfully. The main advantage of this method is that, once analysis of simulations is finished, fast computations can be done to test various systems. Such theoretical information is necessary for each array before being used in a bigger network of devices to collect useful data.

2. Methodology

2.1. Simulations and Data

The study is entirely based on Monte Carlo data, obtained with CORSIKA (COsmic Ray SImulations for KAscade) [8], which is a widely used program for simulations of cosmic-ray cascades, initiated by various particles. It is able to use 50 types of particles, including leptons, hadrons, resonance states, corresponding antimatter as well as nuclei with the atomic mass up to 56. Particle tracking takes place in the atmosphere consisting of nitrogen (78.1%), oxygen (21.0%) and argon (0.9%), where primaries interact, decay, and produce secondaries. Earth atmosphere is divided into five layers which allow for describing differences in the air density at specific altitudes. The program provides secondary particles by their ID number, trajectory, Lorentz factor, time from the first interaction as well as their Cartesian coordinates [8].

In the presented study, simulations are performed using CORSIKA 7.7100 from October 2019 [9]. For hadronic interactions at high energies, the EPOS-LHC [10] model is used, which stands for the *Energy conserving quantum mechanical multiscattering approach, based on Partons, Off-shell remnants and Splitting parton ladders*. This model takes into account heavy-ion data obtained by RHIC and LHC, and it uses some corrections which allow for achieving high energies as well as consistent, accurate results. In order to simulate hadronic interactions at low energies, URQMD (*Ultra-relativistic Quantum Molecular Dynamics*) [11,12] routines are used. It is a universal tool, including various heavy-ion interactions, for instance fragmentation processes, collective flow or correlations between interactions.

Electromagnetic interactions are usually simulated using an NKG [13,14] (Nishimura-Kamata-Greisen) option which provides a more analytical approach and does not require a full Monte Carlo. The main advantage is the reduction of simulation time, but, on the other hand, this option gives only general information about the electromagnetic component, mainly the total number of electrons at a specific altitude. Such properties like accurate location, momenta, and arrival time are lost. In the presented study, for more accurate treat-

ment of electromagnetic subshowers, the EGS4 [15] model is used, which stands for *Electron Gamma Shower system version 4*. This approach results in significantly longer execution time but enables simulating all electromagnetic particles with needed information. It should be noted that CORSIKA in the described version uses EGS4 with some modifications, namely the mean free path is implemented referring to density changes at different altitudes, and the formula for ionisation losses in the atmosphere has also some corrections.

Monte Carlo samples are comprised of EAS with a wide range of primary cosmic-ray particle energies starting from 1 TeV. Cascades generated by particles with lower energies contain so few particles reaching the ground that they should be included in the flux of uncorrelated background. There are eighteen chosen primary energies, from 1 TeV up to 4000 TeV, which are adjusted to increase approximately logarithmically and including the integer powers of ten. CORSIKA simulations are repeated not only at different energies, but also for different primaries: protons, photons, alpha particles, and N, Si, Fe nuclei. First, the data set includes EAS perpendicular to the Earth surface (with zenith angle $\theta = 0^\circ$), and another data set is comprised of EAS reaching the surface at seven selected zenith angles, from 10° to 70° with a step of 10°. In the case of azimuthal angle φ, in every case, it covers the whole range (0°–360°). Energy cuts for secondary particles are chosen separately for hadrons (0.3 GeV), muons (0.3 GeV), electrons (0.003 GeV) and photons (0.003 GeV). Such minimal values of energies were chosen for certain reasons. The number of muons produced in the showers, whose energy is lower than 0.3 GeV, is negligible. In the case of electrons and photons, this is approximately minimal energy for them to penetrate 1 mm of aluminium, which should correspond to the detector enclosure. In this work, all simulations and calculations were performed at a single altitude—sea level. In the future, dependence on altitude needs to be introduced, even if one may expect that the majority of CREDO detectors will be operating in the most populated areas, which are concentrated in the 0–200 m above the sea level range.

2.2. Data Analysis

The first step in the analysis is to characterise EAS using information extracted from simulations. The easiest way to do this, for the purpose of this study, is by defining the function of particle density ρ, parameterised separately for different types of primary cosmic-ray particles. In this work, it has four parameters: the energy of the primary particle, E, the distance from cascade axis (i.e., extrapolated direction of the primary cosmic-ray particle), r, the zenith angle of the primary particle approach direction, θ, and the total number of produced particles, N_{part}, reaching the ground. For simplification, it was assumed that cascades are circularly symmetrical around the cascade axis. Another simplification was made about the time at which particles from EAS arrive on the ground. The time interval between the first and last particle that reaches the ground is of the order of 100s of nanoseconds. This is less than the coincidence time window in the test system, so any time differences within a cascade can be neglected. Each of the mentioned quantities was analysed more or less exhaustively, and pre-defined functions were fitted to data.

The particle density ρ function can be described as a product of several factors given by the following formula:

$$\rho\left(r, \theta, E, N_{part}\right) = \rho_{norm}(r) \cdot F_\theta(\theta) \cdot F_E(E, r) \cdot F_N\left(N_{part}, r\right) \quad (1)$$

where:

- $\rho_{norm}(r)$—is a function which defines the standard "profile" of the footprint of the cascade. It represents relation between particle density and distance from the centre of the shower. This function is fitted for vertical cascades of a chosen energy. It is assumed that particle density for cascades with different energies or other parameters are generally similar but need corrections which depend on parameters of the cascade considered. The following factors $F_\theta(\theta)$, $F_E(E, r)$, and $F_N\left(N_{part}, r\right)$ are normalised to unity for the "standard" cascade and provide correction to the particles density

if the parameters of a cascade are different. Figure 1 presents the shape of this distribution for different types of particles in the shower.

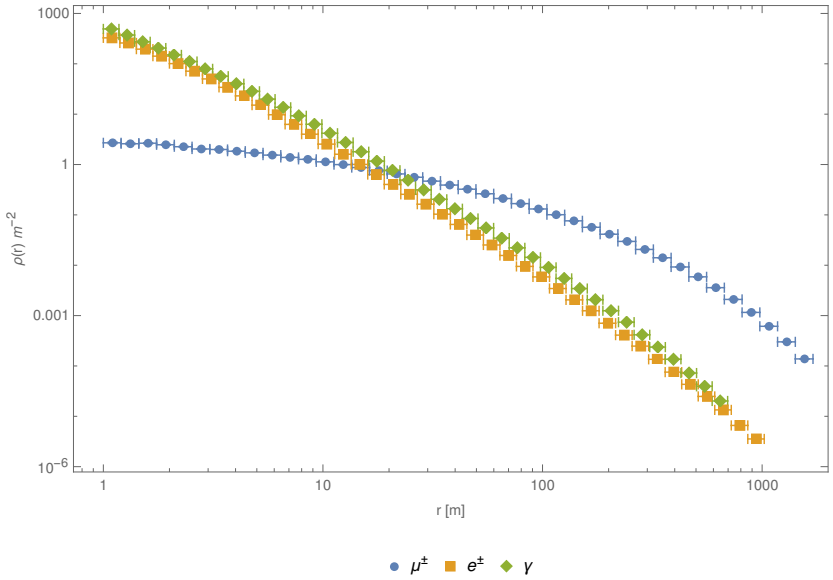

Figure 1. $\rho(r)$ distribution of muons, electrons & positrons and photons from cascades initiated by protons with energy E = 4000 TeV, arriving at the zenith angle $\theta = 0^{\circ}$, as a function of the distance to the shower axis, r.

- $F_E(E, r)$—is a factor which defines how much the density of secondary particles is changing with the energy of the primary cosmic-ray particle. It affects not only the normalised density but also modifies the dependence on the distance r. The two-dimensional function presented in Figure 2 is smooth and can be easily parameterised.

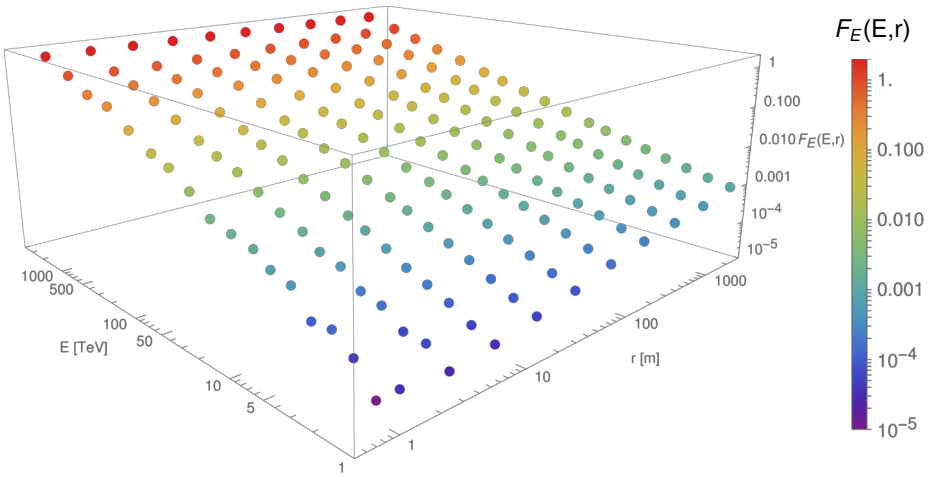

Figure 2. Scaling factor $F_E(E, r)$ normalised to unity for E_{norm} = 4000 TeV as a function of the distance r and energy E, obtained for vertical cascades initiated by cosmic-ray protons.

- $F_N\left(N_{part}, r\right)$—the number of particles produced in the shower which reach the ground level, N_{part}, is strongly correlated with the (unknown) altitude at which the cascade started to form. Thus, depending on the actual development of the cascade at a given energy, not only the total number of particles fluctuates around average $\langle N_{part} \rangle$, but also the dependence on the distance r is slightly changing. This factor relates fluctuations in the total number of produced particles with a density profile of the EAS. Figure 3 presents the correction which needs to be applied to account for this effect.

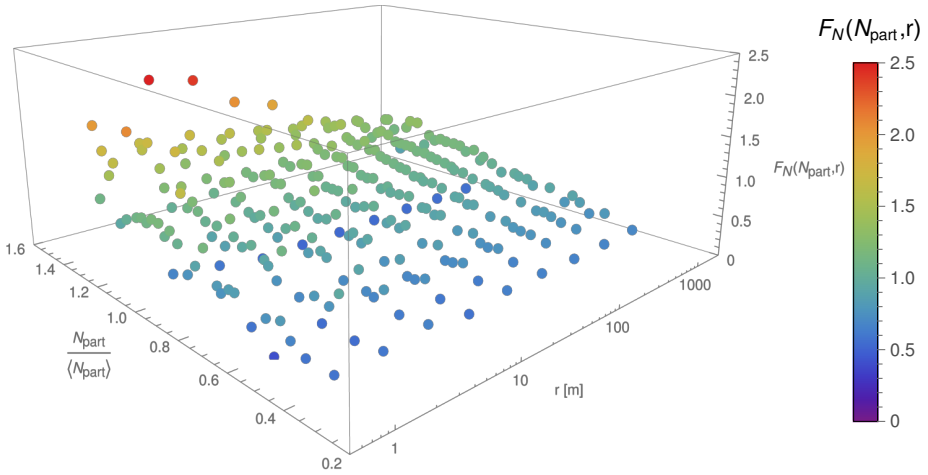

Figure 3. Scaling factor $F_N(N_{part}, r)$ as a function of the distance r and the ratio of the number of secondary particles reaching the ground and the average number of them for given energy, $N_{part}/\langle N_{part}\rangle$, obtained for vertical cascades initiated by protons with the energy $E = 4000$ TeV.

- $F_\theta(\theta)$—is a factor which relates the secondary particle density with the zenith angle of the primary cosmic-ray particle. Considering only geometrical effects for a flat detector on the ground, it should decrease as $cos(\theta)$. However, the way in which the angle of incidence modifies particle density on the ground is more complicated, as it is affected by the varying thickness of the atmosphere. This was analysed only briefly, assuming that, for fixed energy, the density changes the same way as the total number of particles reaching the ground. Figures 4 and 5 present this relation. A function fitting this dependence and the $cos(\theta)$ dependence from simple geometrical considerations are the two alternatives considered in the analysis.

Details about forms of used functions are presented in Appendix A.1. All of the previously defined relations were fitted separately for different types of primary cosmic rays and for three components of shower particles: muons, electrons+positons and photons, with minimal energies the same as described in Section 2.1. Other types of secondary particles were ignored due to their negligible contributions. This division was chosen because of different properties of these particle types and resulting from their different behaviour in various types of detectors and the process of cascade development. Figures 6–8 compare $\rho(r)$ distribution of different components of EAS for different primary cosmic rays.

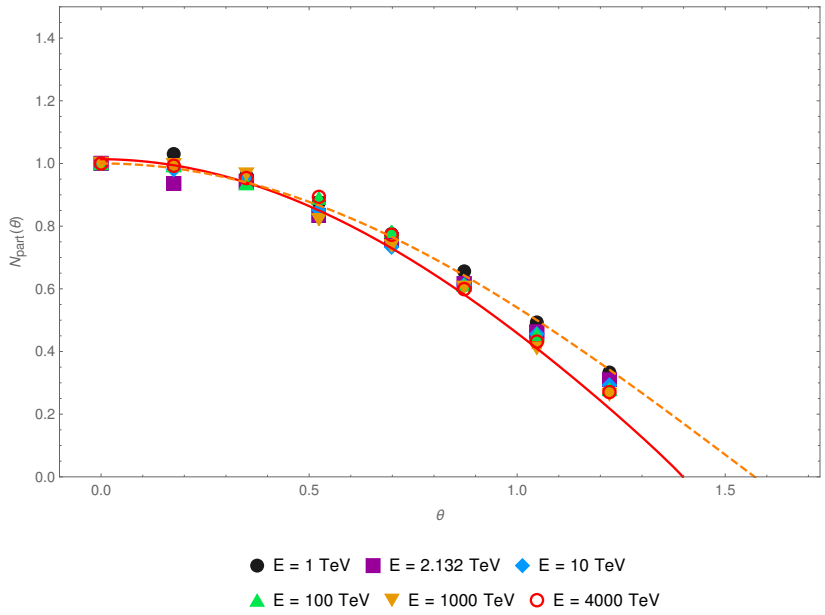

Figure 4. Normalised relation $N_{part}(\theta)/N_{part}(0)$ with fitted scaling factor $F_\theta(\theta)$ (red solid line) for muons in cascades initiated by protons. It shows how the number of secondary particles which reach the ground changes with an increasing angle of incidence of primary cosmic-ray particles. The dashed line represents the $cos(\theta)$ function. For clarity of the picture, only selected energies are shown.

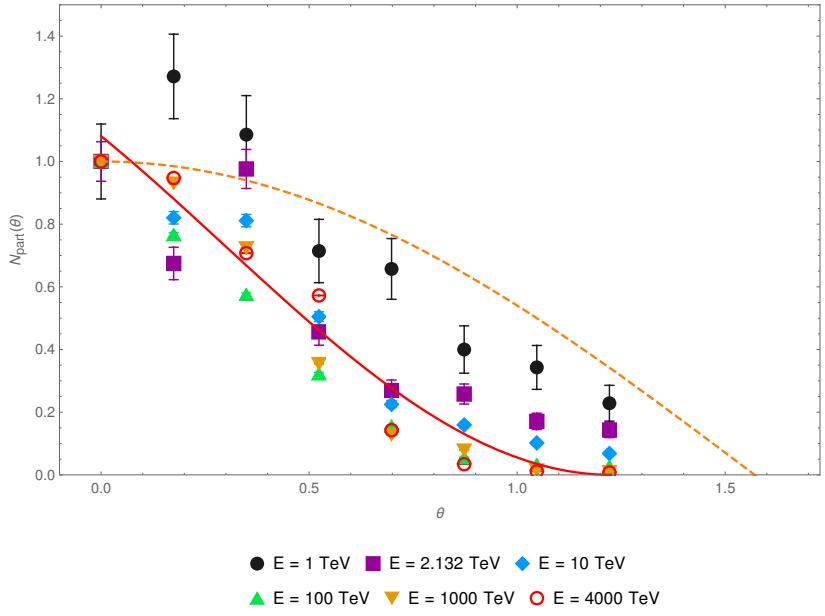

Figure 5. Normalised relation $N_{part}(\theta)/N_{part}(0)$ with fitted scaling factor $F_\theta(\theta)$ (red solid line) for electrons in cascades initiated by protons. It shows how the number of secondary particles which reach the ground changes with an increasing angle of incidence of primary cosmic-ray particles. The dashed line represents the $cos(\theta)$ function. For clarity of the picture, only selected energies are shown.

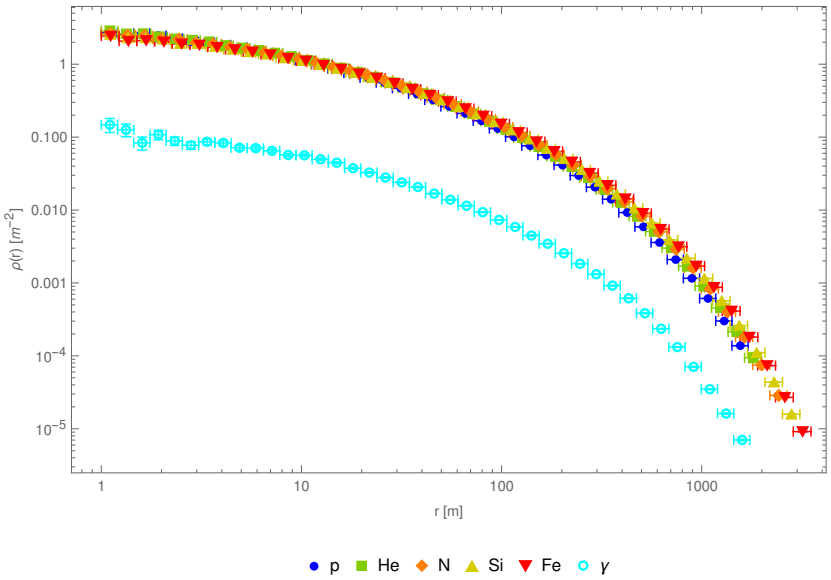

Figure 6. $\rho(r)$ distribution of muons in cascades initiated by different primary cosmic-ray particles with energy $E = 4000$ TeV.

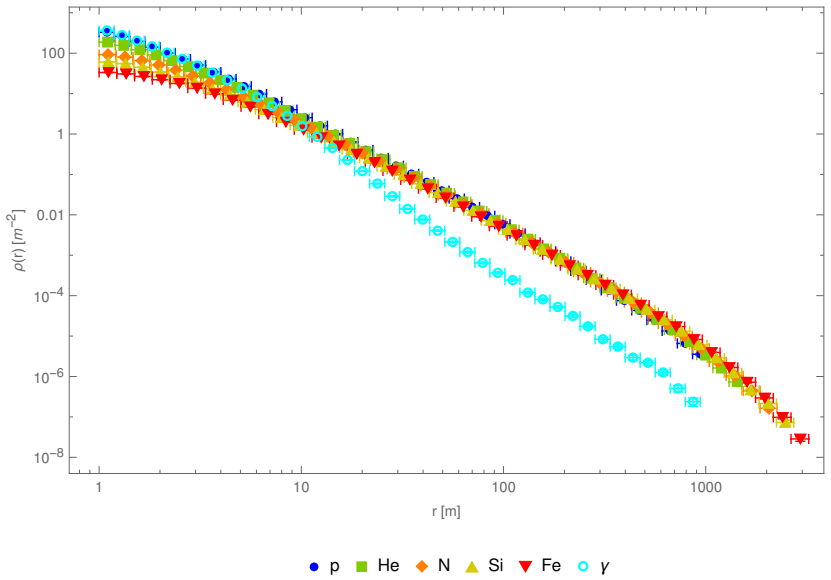

Figure 7. $\rho(r)$ distribution of electrons/positrons in cascades initiated by different primary cosmic-ray particles with energy $E = 4000$ TeV.

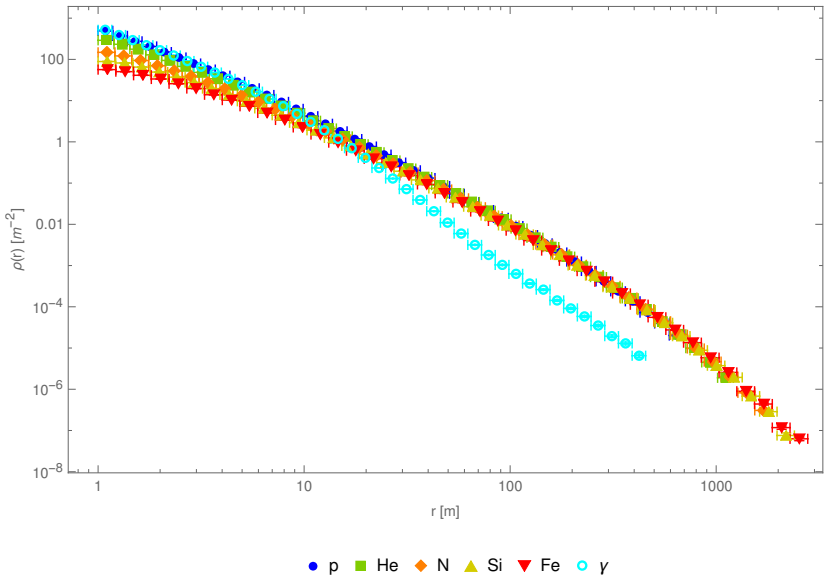

Figure 8. $\rho(r)$ distribution of photons in cascades initiated by different primary cosmic-ray particles with energy $E = 4000$ TeV.

Even for a fixed energy of the primary cosmic-ray particle, the number of particles, N_{part}, reaching the ground may vary significantly, depending on details of cascade development. In Figures 9 and 10, the examples of distributions of the number of muons and electrons are presented, respectively. By analysing simulated data, one can see that, for muons produced in an EAS, the distribution of their number can be described by a Gaussian function. For electrons and photons, the shape of such distribution is very different. Fortunately, in this case, the logarithm of the number of produced particles happens to fit Gaussian distribution. Both of its parameters μ and σ are functions of the energy of primary particle as described in more detail in Appendix C. Furthermore, in place of the distribution of the number of particles, the functional form $f(N, E)$ is used. The results of such fits are shown in Figures 9 and 10. In the counting of the number of particles, for the purpose of the calculation of the probability of detection of an EAS, it is sufficient to consider only those which are within some range of distances from the cascade centre. At large distances, the chance of detection becomes negligible, and the determination of the limit is described in detail in Appendix B.

Knowing all properties of various cosmic-ray cascades described in this section, it is possible to go to the next step—analysis of signals which EAS can leave in a certain type of detector.

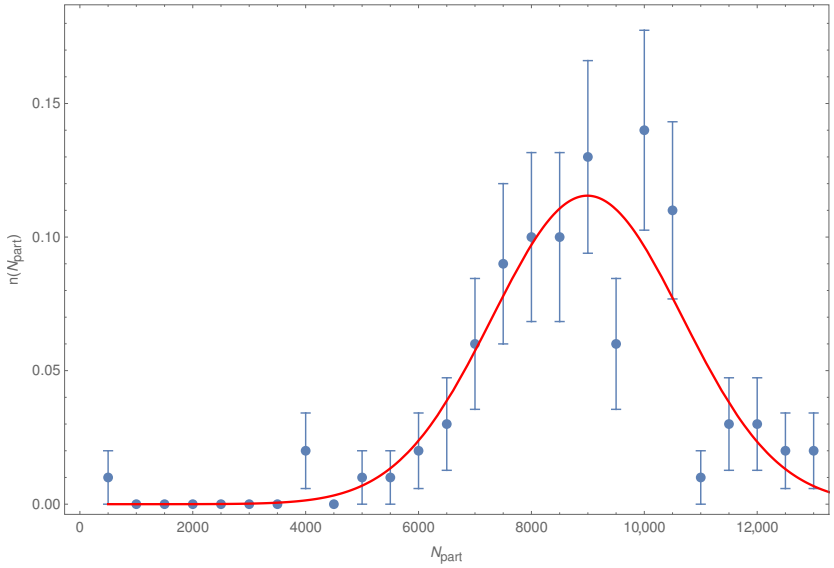

Figure 9. Probability distribution of the number of muons in cascades initiated by protons with energy $E = 1000$ TeV. The line is the fitted Gaussian function.

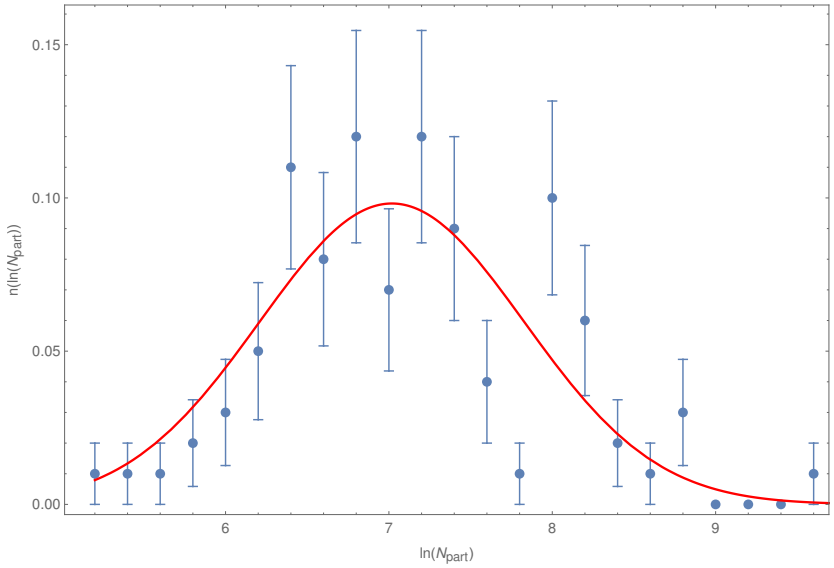

Figure 10. Probability distribution of the logarithm of the number of electrons in cascades initiated by protons with energy $E = 1000$ TeV. The line is the fitted Gaussian function.

2.3. Background Estimation

The first task of the analysis is the evaluation of the flux of background particles and probability of fake signals i.e., not caused by an EAS. In this study, only those cascades which originate from cosmic-ray particles with energy of at least 1 TeV are considered as EAS. At lower energies, the number of secondary particles becomes so low that the probability of detecting more than one of them in a small detector system becomes negligible, thus it was assumed that they are included in the uncorrelated background. This study focuses on the scintillator detectors, which for the simplification are flat, placed horizontally on the ground and are characterised by only four parameters. The first of them is the area of the detector A, while the thickness is assumed to be negligible. The second is the measurement time δT, defined as the time interval after a particle hits the detector during which any other particles can not cause a second signal. Other two quantities are efficiency η of the detector and frequency of fake signals f_f which can be caused, for example, by the noise in the electronics. These last two properties should be determined

experimentally for each detector type, and the efficiency may depend on the energy and type of the particles entering the detector. In this work, the *background* includes both uncorrelated, single cosmic-rays which come from all directions with constant flux indicated as I_{bg} and fake signals.

For infinitely short measurement time dT, the probability of at least one signal from any background source to happen is $dT(\eta \cdot A \cdot I_{bg} + f_f)$, but, for any longer time δT, the correct formula is:

$$P_{bg} = 1 - \exp\Big(-\delta T\Big(\eta \cdot A \cdot I_{bg} + f_f\Big)\Big) \tag{2}$$

2.4. Cosmic-Ray Energy Spectra

To evaluate the possibility of registering a signal from an EAS in a detector system, one needs to know the spectrum of primary cosmic-ray particles including high-energy photons. In this work, rather than account for all possible particle types, six representative groups are analysed: protons, four for nuclei and photons.

The frequency with which they enter the Earth's atmosphere is denoted as $j_i(E)$ and depends only on the energy E of the primary particle and its type i. For protons and nuclei, it is described by a simple power law:

$$j_i(E) = j_{0,i} E^{-\gamma} \tag{3}$$

where $j_{0,i}$ is a constant for a certain type of primary nuclei, and the slope parameter γ has one of two different values below and above the energy region called "the knee".

The energy spectrum of cosmic rays was extensively studied by various experiments over the last several decades [16,17]. However, at energies above several dozens of TeV, the exact shape of the spectrum for different types of nuclei is not so well known, due to difficulty in identification of the primary particle type. High energy cosmic rays are studied mostly in experiments carried on the surface of the Earth, which can easily distinguish EAS caused by photons and those caused by protons or nuclei, but determination of the mass of the nuclei is impossible or very difficult. Thus, in this study, five groups of primary nuclei are used: protons, p, helium nuclei He, light nuclei represented by nitrogen N, medium represented by silicon Si, and the heaviest nuclei represented by iron, Fe. Flux rates for other nuclei are added to those of the representative nuclei which are closest in mass. The cosmic-ray spectrum can be divided into two regions, below the "knee" and above it. While the location in energy of the "knee" for different nuclei is not well known, it is commonly accepted that it moves to higher values for heavier nuclei. One can assume that the slope parameter γ has the same values for all nuclei while the positions of the "knee" for different nuclei groups may be treated as free parameters, adjusted to reproduce the well known energy spectrum for all cosmic-ray particles [16]. Spectra estimated this way for five groups of primary cosmic-ray nuclei are presented in Figure 11. The simple functional representation is convenient in the calculations described in the next section.

In the case of photons, it is hard to define a diffusive gamma rays flux because most of them originate from some point-like sources scattered over the entire sky. However, even if gamma ray frequency is different in different regions of the sky, for longer measurement time, the flux is observed on the Earth averages. A rough spectrum for photons can be obtained if some ratio of frequency of high energy photons to the total flux of cosmic rays is presumed [18]. In this work, it was assumed that, for energies of about 1 TeV, there is about 1 high energy photon per 10 nuclei, and this ratio drops to $1 : 10^4$ at $E = 10^6$ TeV [16]. A comparison of gamma rays and other cosmic-ray spectra is shown in Figure 12.

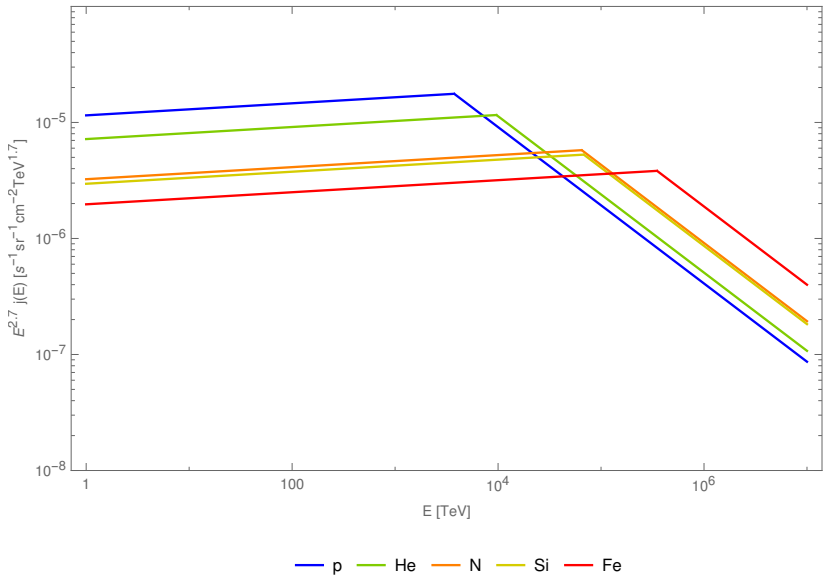

Figure 11. Parameterised differential energy spectrum for representatives of primary cosmic-ray nuclei used in this work.

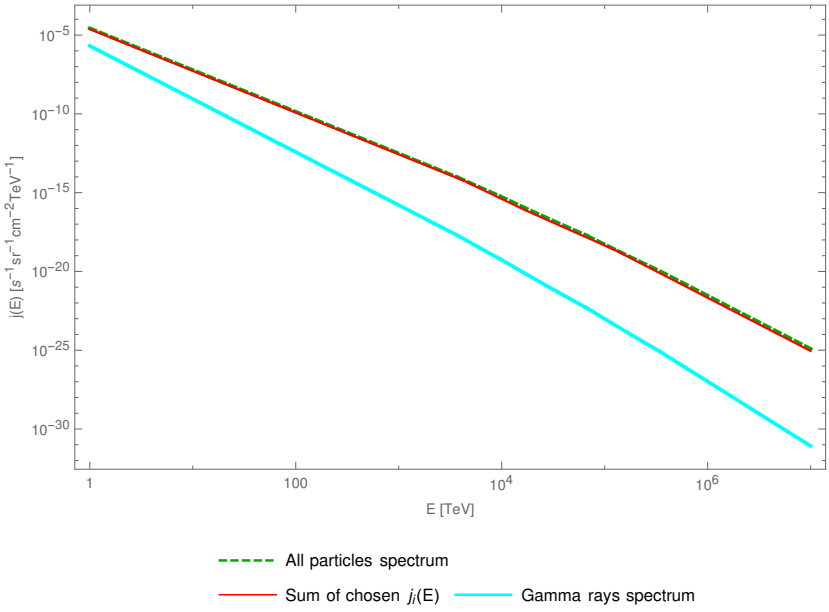

Figure 12. Parameterised energy spectra of all cosmic-ray nuclei [19] (dashed line), sum of energy spectra of five representative nuclei used in this work (orange line) and the energy spectrum of gamma rays [16].

2.5. Signal Estimation

Considering any individual cosmic-ray cascade, the probability of registration of a signal in a single detector from at least one particle is:

$$P = 1 - \exp\left(-\eta \cdot A \cdot \rho\left(r, \theta, E, N_{part}\right)\right) \tag{4}$$

where the secondary particle density depends not only on the parameters explicitly mentioned, but also on the primary cosmic-ray particle. In a general case, the probabilities P_j for each device j may be different because the properties of detectors are not always identical but also because the the particle density in the locations of the detectors may be different. For detection of an EAS, it is necessary to require the coincidence of a few signals

in systems consisting of several devices. The general formula for probability of registering k signals in n detectors is the following:

$$Q(P_1, ..., P_n, n, k) = \sum_{\substack{A \subset \{1,...,n\} \\ |A|=k}} \left(\prod_{j \in A} P_j \right) \left(\prod_{j \in \{1,...,n\} \setminus A} (1 - P_j) \right), \tag{5}$$

where all combinations of k detectors from n detectors are considered. However, if the detectors are identical and the distances between them are very small, the probability P for each of them may be treated as the same. In this case, the probability of a multi-signal event with k signals registered by a system of n devices is described by binomial distribution:

$$Q(P, n, k) = \binom{n}{k} P^k (1 - P)^{n-k} \tag{6}$$

To evaluate the expected number of events caused by Extended Air Showers during some period of time, an integration over distribution of the number of produced particles, N_{part}, area around the devices, ϕ and r, zenith angles, θ, and all energies of primary cosmic-ray particles, for all types of them, must be performed. In general, if the distances between devices are not negligible, particle density from the shower for each one of them is different. In such a case, integration over the area around the array could be performed using Cartesian coordinates on a plane x and y. Then, knowing the exact positions of each detector, the distance to the shower axis r for each of them is calculated and used to obtain particle density ρ and probability P. When small detectors are placed very close together, as in the test system, all detectors can be treated as placed at exactly the same location, and Equation (6) can be used. Then, the assumption that cascades are circularly symmetrical reduces the integral over the surface and can be reduced to the integral over radial distance, while the integration over azimuthal angle is reduced to the factor $2\pi r$. The integration over the distance of the cascade from the detectors, r, is limited by certain radius r_{max}, which was mentioned previously and is better described in Appendix B. Limits of the integral over the number of particles in the shower, N_{min} and N_{max}, are taken from N_{part} distributions as $N_{min} = \langle N_{part} \rangle(E) - 3\sigma_N(E)$ and $N_{max} = \langle N_{part} \rangle(E) + 3\sigma_N(E)$. Considered energy range starts at $E_{min} = 1$ TeV and ends at $E_{max} = 10^7$ TeV above, for which the cosmic-ray flux is too small to expect any such EAS in a reasonable measurement time. The expected number of events for each primary cosmic-ray particle type is thus computed as:

$$\langle N(n,k) \rangle_i = \int_{E_{min}}^{E_{max}} \int_0^{\frac{\pi}{2}} \int_0^{r_{max}} \int_{N_{min}}^{N_{max}} T Q(n,k,P) 2\pi \, r \, j(E) f(N,E) \, dN \, dr \, d\Omega \, dE \tag{7}$$

where T is the time during which the measurement is performed, P is a function of all variables which are integrated and $f(N, E)$ represents the probability distribution that N secondary particles from a cascade with the energy E reach the ground, and i denotes the type of the primary cosmic-ray particle.

3. Results

This section presents the results of calculations for a system of four simple CosmicWatch [20] detectors that were used in the test of EAS measurement [21]. All parameters which were assumed for these detectors are described in Appendix D, but the most important information is that the system consisted of four devices placed very close to each other, and the duration of measurements was one week. The most precise description of these data should be obtained when the particle density is calculated using all correction factors present in Equation (1). In order to see how important each of these corrections is, several models with simplifications are presented, in which other forms of F_θ and $F_N(N_{part}, r)$ are used. These two functions are modified as they are least precisely determined from the simulations. In addition, a very crude model based solely on dependencies found in published papers is also considered:

- **Model 1**—the basic version which uses functions fitted to results of simulations and presented in Figures 1–5;
- **Model 2**—in place of F_θ dependence obtained from the fit, the simple geometrical correction $F_\theta = cos(\theta)$ is used, in order to estimate how large change related to the zenith angle dependence may be expected;
- **Model 3**—in place of complicated version of $F_N(N_{part}, r)$ a simple linear approximation is used:
  $F_N(N_{part}, r) = F_N(N_{part}) = N_{part}/\langle N_{part}\rangle$,
  which changes the normalisation but does not modify the dependence on r;
- **Model 4**—uses both simplified versions of the functions $F_\theta = cos(\theta)$ and linear version of $F_N(N_{part})$;
- **Model 5**—uses particle density defined as a function of distance r and the number of particles which reach the ground N_{part} only—a commonly accepted approximation for muons [17], described in details in Appendix A.2. As the appropriate function for electromagnetic component of EAS is not available in [17], the same functional form as for muons is used (even if it is obviously not accurate). The particle density is then modified by a scaling factor $F_{theta}(\theta) = \cos(\theta)$ described earlier.

Models 2–5 must not be treated as alternatives to Model 1, their assumptions are less accurate and they were introduced to show how large modifications of results may be expected. Comparison of results of calculations for the background and in these models is presented in Table 1. The numbers for background were obtained using the probability from Equation (2) to find probabilities of appropriate coincidences which are then multiplied by the number of possible measurement times δT during the whole measurement period of one week. The expected number of single signals (i.e., events with a registered signal in only one of the four detectors) from the background is much larger than that from high-energy cascades considered in the calculations, but already probability of a coincidence of two out of four detectors is much smaller in the case of background than for calculations in any model considered. It is also clear that the change of assumptions regarding the form of F_θ or $F_N(N_{part})$ are important as they may change the results by a factor of more than 10. In addition, a simplified model of primary particles spectrum was used (presented in Section 2.4). Composition of primary cosmic-rays was measured in satellite experiments precisely for energies in the range from 1 to 100 TeV [22,23], and some structures in the spectra were found. As these structures were not precisely reproduced in the cosmic-ray spectra used in the model, the possible systematic modification of presented results was tested by increasing and decreasing the cosmic-rays flux by a factor of 2 in this energy range. The maximal difference in the number of expected events is around 30% for two-fold coincidences, 6% for three-fold coincidences, and less than 1% for four-fold coincidences.

Table 1. Number of events with k = 1–4 signals in the system of four detectors expected from the background and predicted by different models for the measurements during one week, with the assumption that all particles from each cascade can reach the detectors.

k	Background	Model 1	Model 2	Model 3	Model 4	Model 5
1	1,168,000	131,100	257,300	159,050	219,600	147,100
2	0.169	779	4414	29.5	164	315
3	1.1×10^{-8}	170	1067	6.1	33.1	125
4	2.6×10^{-16}	78	541	3.9	20.2	132

The numbers presented in Table 1 can not be directly compared to the results of measurement [21], as the calculations did not take into account all conditions in which this measurement was performed. In particular, the detectors were working inside the building close to a window. Muons are able to penetrate through the roof and walls, while the electromagnetic component of the shower is largely stopped there, so the electrons and photons are able to reach the detectors only if they enter through the window. To mimic this

behaviour in the model calculations only, 1/6 cascades with $\theta > 15^\circ$ had an electromagnetic component included. Factor 1/6 comes from taking angular width of the window $\phi = 60^\circ$. This is a crude approximation of the experimental conditions, but allows for comparing results of modified calculations with the measurements in Table 2. Such correction was not applied for the background, as it is not clear what the ratio is of muons to electrons and photons in it; thus, only the numbers from Table 1 were repeated as the upper limits. The standard Model 1 gives a similar number of $k = 2$ coincidences but predicts an order of magnitude larger number of $k = 3$ and $k = 4$ coincidences. Other models deviate even more from experimental measurements, which is not a surprise, as, in their assumptions, more simplifications are included. Differences of this size can be anticipated as little is known about the efficiency of detectors for different particle types. The discrepancies clearly indicate that some properties of the detectors do not agree with model assumptions.

Table 2. Number of events with k = 2–4 signals in the system of four detectors measured during one week and compared to the expectations from the background and predictions from different models, with the assumption that electrons and photons from a cascade can reach the detectors only if they enter into the building through a window.

k	Events	Background	Model 1	Model 2	Model 3	Model 4	Model 5
2	94	<0.169	130	736	5.39	27.9	53
3	2	$<1.1 \times 10^{-8}$	28.5	178	1.03	5.55	21
4	1	$<2.6 \times 10^{-16}$	13	90	0.66	3.37	22

It was also studied how changing the considered area around the system, decreasing r_{max} in integral in Equation (7), modifies final results. It was found that it has little impact as only a relatively close occurrence of an EAS, within $r_{max} \approx 25$ m around the devices, has a chance of causing a coincidence signal. However, it is not a surprise that the effective area in which such small detector system can register a typical EAS is small. Larger showers are naturally more likely to cause events with a greater number of coincidences, but they are also far less frequent. With these kinds of calculations, it is possible to depict how many of the total number of expected events should be caused by cascades of certain energy. In Figure 13, it can be seen that cascades with energy below 10 TeV produce mostly single signals, while the coincidences with signals in all four detectors are most probably due to cosmic-ray cascades with energies between 10^3 TeV and 10^5 TeV.

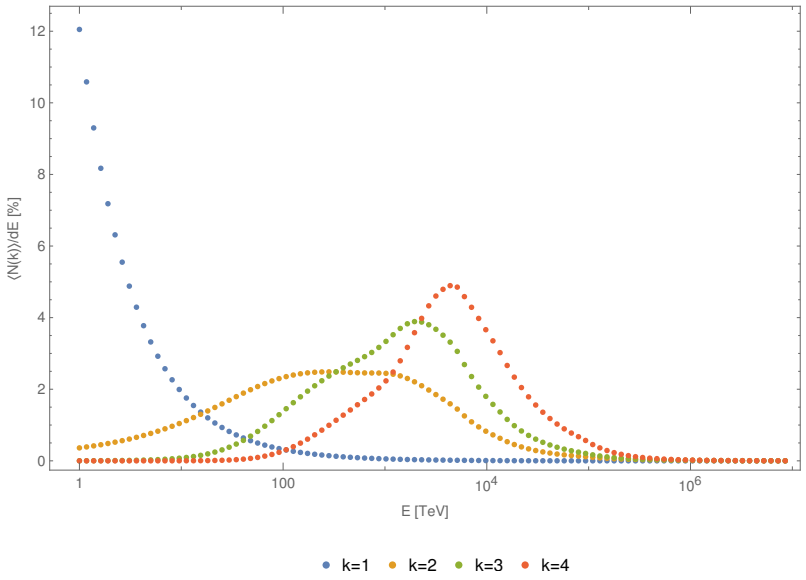

Figure 13. Percent of events per energy range for different number of coincidences k for considered system. This plot was made for model nr 1 with window modification included.

4. Photon Cascades

The system of four detectors with a small area is sufficient to detect cosmic-ray cascades, but does not provide much information on their properties. It is obvious without any calculation that systems consisting of more elements allow for detecting cosmic-ray cascades more efficiently and may provide more information on the primary cosmic-ray particle. Multiple coincidences of signals in more than four detectors indicate higher energy of the observed EAS. An interesting opportunity may be provided if some of the detectors in the system can detect electromagnetic components of the shower while the others are sensitive to muons only. Such methods were used to distinguish gamma-rays from cosmic-rays in many experiments like CASA-MIA [24] and KASCADE [25]. In the case of the presented exemplary array, it may be achieved by appropriate shielding of some devices, such that electrons and photons are stopped before reaching the scintillator. As it can be seen in Figure 6, the number of muons in cascades initiated by primary photons is one order of magnitude lower than in cascades with the same energy but initiated by other primary cosmic-ray particles. Quite the opposite, the number of electrons/positrons (Figure 7) and photons (Figure 8) is the largest in the photon initiated cascades. A signature of a photon EAS would be thus observation of many signals in elements detecting electromagnetic components and a lack of signals in those sensitive to muons only. Such system would need detectors larger than CosmicWatch, and the design of optimal setup of the system requires additional studies which may be performed in the future using methods described in this work.

5. Conclusions

The analysis of simulations from the CORSIKA program for different incoming cosmic-ray primary particles in a wide range of their energies enables determining how the particle density observed on the ground changes with the distance from the centre of the cascade for several cascade parameters. Such complicated multi-dimensional dependence can be approximately factorised using several functions which are fitted with analytical formulas. Integration of the particle density function over the cosmic-ray spectrum allows for calculating the probability of registering a signal from an EAS in the detector. This method was applied to a system of four small detectors and compared with results of measurements [21]. It was found that, even if uncertainties of the calculations are still large, the hypothesis that Extensive Air Showers were observed was confirmed. This ensures that small and not sophisticated, therefore inexpensive, systems may provide valuable measurements and can be successfully applied within the CREDO project. Slightly larger and more complex, but still relatively small detector systems may provide identification of cascades initiated by high energy cosmic-ray photons.

Author Contributions: Conceptualization, J.S.P., K.W.W., P.H.; data curation, W.S.; resources, K.R., T.S.; formal analysis, J.P., W.S.; methodology, J.P.; project administration, P.H.; writing—original draft preparation, J.P., W.S., K.W.W.; software, J.P., W.S.; supervision, K.W.W.; writing—review and editing, W.S., P.H., K.A.C., Ł.B., M.P., S.S., T.W., O.B., T.S., K.R., A.T., D.A.-C., M.N. All authors have read and agreed to the published version of the manuscript.

Funding: This research received no external funding.

Institutional Review Board Statement: Not applicable.

Informed Consent Statement: Not applicable.

Data Availability Statement: The data presented in this study are available on request from the corresponding author. The data are not publicly available due to their storage on ACC Cyfronet AGH-UST servers.

Acknowledgments: The authors acknowledge the leading role of the CREDO Collaboration in preparation of this research and the commitment made by the Institute of Nuclear Physics Polish Academy of Science. This study has also been supported by PLGrid Infrastructure. The authors would like to thank the ACC Cyfronet AGH-UST for their supercomputing support.

Conflicts of Interest: The authors declare no conflict of interest.

Abbreviations

The following abbreviations are used in this manuscript:

EAS	Extensive Air Shower
CREDO	Cosmic-Ray Extremely Distributed Observatory
CRE	Cosmic-Ray Ensembles

Appendix A. Versions of ρ Function

Appendix A.1. Fitted Factors

Here, the functions used to describe factors in Equation (1) are presented. Two of them, $\rho(r)$ and $F_\theta(\theta)$, are functions of only one parameter so fitting them is not a big issue. In the case of other two factors, the $F_E(E,r)$ and $F_N(N_{part},r)$ fitting procedure was performed in two stages. Firstly, their dependence on only E or N_{part}, respectively, for different fixed distances r, was fitted and then parameters of such one-dimensional functions were treated as some functions of r. Forms of all functions are listed in Table A1, where parameters denoted as A, B, C, a, b, c, etc. have different values in each function.

Table A1. Forms of functions used to define factors in $\rho(r,\theta,E,N_{part})$ relation.

Factor	Form of the Function	Form of Parameters Functions
$\rho(r)$	$\exp\left(A+Br^C\right)$	-
$F_\theta(\theta)$	$A(\cos(B(\theta+C)))^D$	-
$F_E(E,r)$	$A(r)\cdot E^{B(r)}$	$A(r)=a\cdot r^b$ $B(r)=a\cdot r^b$
$F_N(N_{part},r)$	$A(r)+B(r)\cdot N_{part}+C(r)\cdot N_{part}^2$	$A(r)=b+a\cdot log(r)$ $B(r)=b+a\cdot log(r)$ $C(r)=b+a\cdot log(r)$

Appendix A.2. Approximation of ρ in Model 5

The simplified Model 5 is based directly on measurements and uses an approximation of ρ(r) derived for muons [17]. There is no data on the function appropriate for electrons, positrons and photons, so also for them the same function was used. Model 5 is introduced to show how sensitive the calculations are to different assumptions in the models. Formula (A1) gives the number of particles per square meter:

$$\rho(N_{part},r)=\frac{1.25N_{part}}{2\pi\Gamma(1.25)}\left(\frac{1}{320}\right)^{1.25}r^{-0.75}\left(1+\frac{r}{320}\right)^{-2.5} \tag{A1}$$

where Γ is the gamma function, N_{part} is the number of produced particles and r is the distance from the centre of the shower.

Appendix B. Distance r_{max} Analysis

In all models, it is assumed that cascades are circularly symmetrical, thus it is sufficient to determine the maximal distance from its centre to define the area that is covered by particles from the shower. Obviously, even if some fraction of particles may be found very far from the axis of the cascade, the detection of an EAS at very large distances becomes less and less probable. It is thus reasonable to parameterise the particle density to some maximal distance, r_{max}, especially as uncertainty of such parameterization is very large at large r. In order to define r_{max}, the radius within which some fraction of all secondary particles is contained, R_{prc}, was studied. It was found that the most appropriate values of this fraction are 95%, that the value of R_{prc} is a function of the EAS energy and it can be

fitted as $R_{prc}(E) = A \cdot E^B$ (Figure A1). One can see that the values of R_{prc} are decreasing with the energy of the cascade. This is due to the fact that the secondary particles produced in an early stage of the cascade are emitted at smaller angles when the primary cosmic-ray particle has larger energy. In addition, the later secondary interactions have the same feature, thus the fraction of particles near the cascade axis is larger at higher energies. This way, even if the absolute number of particles at large radius r is growing with the energy, the mean values of r and also R_{prc} are decreasing.

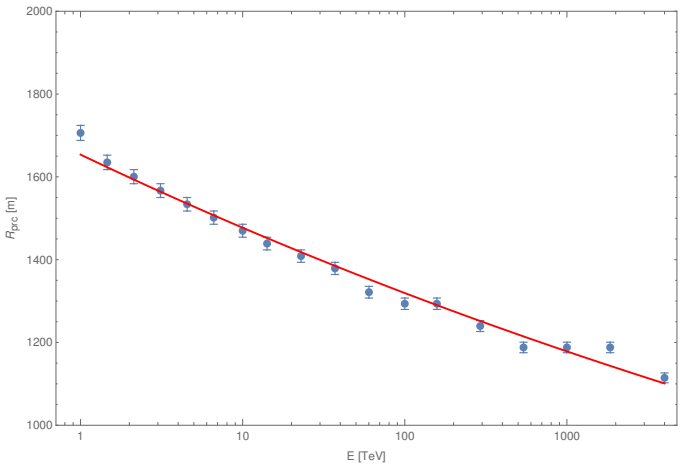

Figure A1. Average distance from the centre of cascade R_{prc} within which 95% of particles produced in the shower initiated by protons are contained.

Appendix C. Parameterisation of the Distribution of the Number of Particles

The Gaussian parameterization was found to describe both the distribution of the number of muons and the distribution of the logarithm of the number of electrons or photons. It has two parameters (μ and σ) which are functions of energy of the primary cosmic-ray particle E. The examples of calculated values of $\mu(E)$ and $\sigma(E)$ for muons are shown in Figures A2 and A3. In order to obtain the probability function $f(N, E)$, used in Equation (7), the parameters of the Gaussian functions for muons are described as functions of the energy of the cascade with a form $10^A \cdot E^B$. In the case of the electromagnetic component of EAS, where the x-axis represented $ln(N_{part})$, functions $\mu(E)$ and $\sigma(E)$ are approximately linear on a logarithmic-linear scale, thus logarithmic functions $A + B \cdot log(E)$ are used. However, in Figures A4 and A5, it can be seen that the energy dependence is more complicated than simple linear approximation, thus extrapolation to higher energies may be inaccurate. This aspect needs additional study in the future.

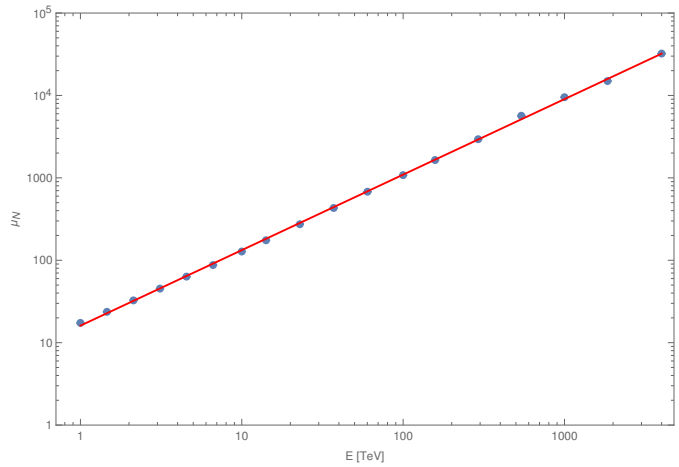

Figure A2. Values of Gaussian distribution parameter μ (for muons) for different energies of the vertical cascades and protons as the primary cosmic-ray particles.

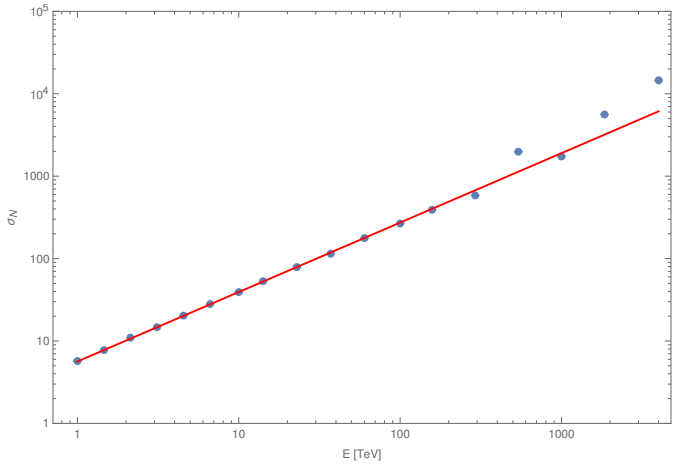

Figure A3. Values of Gaussian distribution parameter σ (for muons) for different energies of the vertical cascades and protons as the primary cosmic-ray particles.

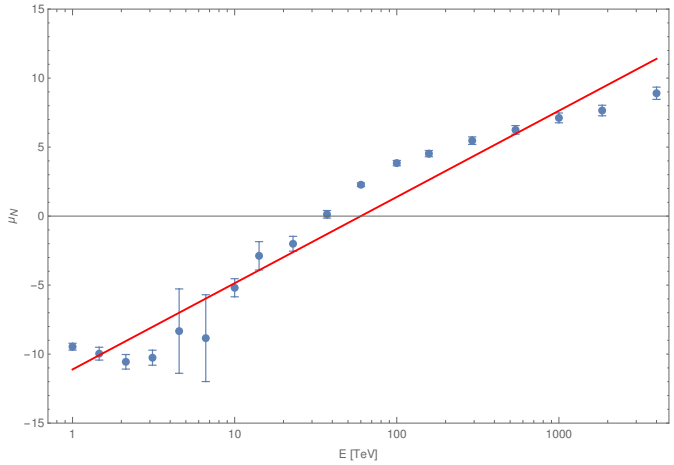

Figure A4. Values of Gaussian distribution parameter μ (for electrons) for different energies of the vertical cascades and protons as the primary cosmic-ray particles.

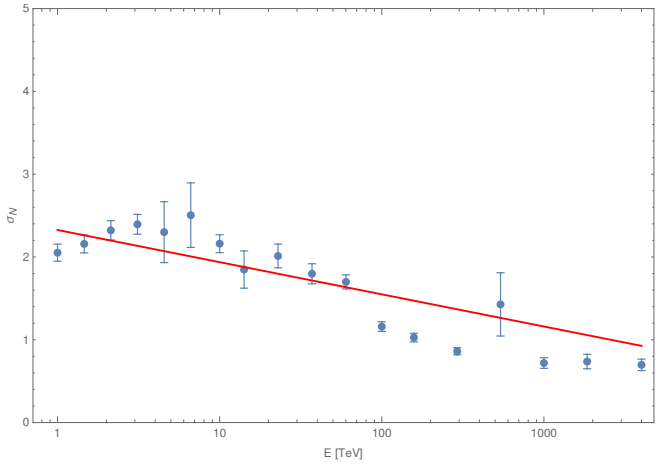

Figure A5. Values of Gaussian distribution parameter σ (for electrons) for different energies of the vertical cascades and protons as the primary cosmic-ray particles.

Appendix D. Detector System Configuration

The tested system [21] comprises four identical scintillator detectors with the active area $A = 25$ cm^2 each and the coincidence time $\delta T = 2 \times 10^{-6}$ s. The detectors were placed within a distance of less than half a meter from each other near windows in a building,

but the geometrical details are not precisely specified. Unknown is the rate of signals from background particles I_{bg}, which depends on sensitivity of the devices to different particle types, and, in addition, it can fluctuate [17]. Quantities like efficiency η and rate of signals from other sources f_f are also not known; thus, in this study, their values were chosen arbitrarily. Efficiency is η = 95% starting from 0.3 GeV for muons and 0.003 GeV for electrons and photons, and the fake signal rate is 0.1 s^{-1} All values of parameters of the tested system [21] used in the model calculations are presented in Table A2.

Table A2. Parameters of the considered system.

Parameter	n	A	δT	I_{bg}	η	f_f
Value	4	25 cm^2	2×10^{-6} s	163 s^{-1} m^{-2}	95%	0.1 s^{-1}

References

1. Homola, P.; Beznosko, D.; Bhatta, G.; Bibrzycki, Ł.; Borczyńska, M.; Bratek, Ł.; Budnev, N.; Burakowski, D.; Alvarez-Castillo, D.E.; Almeida Cheminant, K.; et al. Cosmic-ray extremely distributed observatory. *Symmetry* **2020**, *12*, 1835. [CrossRef]
2. Smith, G.R.; Ogmen, M.; Buller, E.; Standil, S. Possible observation of a burst of cosmic-ray events in the form of extensive air showers. *Phys. Rev. Lett.* **1983**, *50*, 2110. [CrossRef]
3. Fegan, D.J.; McBreen, B.; O'Sullivan, C. Observation of a burst of cosmic rays at energies above 7×10^{13} ev. *Phys. Rev. Lett.* **1983**, *51*, 2341. [CrossRef]
4. Dhital, N.; Homola, P.; Alvarez-Castillo, D.; Góra, D.; Wilczyński, H.; Cheminant, K.A.; Poncyljusz, B.; Mędrala, J.; Opiła, G.; Bhatt, A.; et al. Cosmic ray ensembles as signatures of ultra-high energy photons interacting with the solar magnetic field. *J. Cosmol. Astropart. Phys.* **2022**, *2022*, 038. [CrossRef]
5. Bibrzycki, Ł.; Burakowski, D.; Homola, P.; Piekarczyk, M.; Niedźwiecki, M.; Rzecki, K.; Stuglik, S.; Tursunov, A.; Hnatyk, B.; Castillo, D.E.A.; et al. Towards A Global Cosmic Ray Sensor Network: CREDO Detector as the First Open-Source Mobile Application Enabling Detection of Penetrating Radiation. *Symmetry* **2020**, *12*, 1802. [CrossRef]
6. Clay, R.; Singh, J.; Homola, P.; Bar, O.; Beznosko, D.; Bhatt, A.; Bhatta, G.; Bibrzycki, Ł.; Budnev, N.; Alvarez-Castillo, D.E.; et al. A Search for Cosmic Ray Bursts at 0.1 PeV with a Small Air Shower Array. *Symmetry* **2022**, *14*, 501. [CrossRef]
7. Wibig, T.; Karbowiak, M. CREDO-Maze Cosmic Ray Mini-Array for Educational Purposes. *Symmetry* **2022**, *14*, 500. [CrossRef]
8. Heck, D.; Knapp, J.; Capdevielle, J.N.; Schatz, G.; Thouw, T. *CORSIKA: A Monte Carlo Code to Simulate Extensive Air Showers*; Forschungszentrum Karlsruhe Report FZKA 6019; Karlsruhe Institute for Technology (KIT): Karlsruhe, Germany, 1998.
9. Heck, D.; Pierog, T. *Extensive Air Shower Simulation with CORSIKA: A User's Guide (Version 7.7100 from October 1, 2019)*; Karlsruhe Institute for Technology (KIT): Karlsruhe, Germany, 2019.
10. Pierog, T.; Karpenko, I.; Katzy, J.M.; Yatsenko, E.; Werner, K. EPOS LHC: Test of collective hadronization with data measured at the CERN Large Hadron Collider. *Phys. Rev. C* **2015**, *92*, 034906. [CrossRef]
11. Bass, S.A.; Belkacem, M.; Bleicher, M.; Brandstetter, M.; Bravina, L.; Ernst, C.; Gerland, L.; Hofmann, M.; Hofmann, S.; Konopka, J.; et al. Microscopic models for ultrarelativistic heavy ion collisions. *Prog. Part. Nucl. Phys.* **1998**, *41*, 255–369. [CrossRef]
12. Bleicher, M.; Zabrodin, E.; Spieles, C.; Bass, S.A.; Ernst, C.; Soff, S.; Bravina, L.; Belkacem, M.; Weber, H.; Stöcker, H.; et al. Relativistic Hadron-Hadron Collisions Ultra-Relativ. Quantum Mol. Dyn. Model. *J. Phys. G: Nucl. Part. Phys.* **1999**, *25*, 1859–1896. [CrossRef]
13. Kamata, K.; Nishimura, J. The Lateral and the Angular Structure Functions of Electron Showers. *Prog. Theor. Phys. Suppl.* **1958**, *6*, 93–155. [CrossRef]
14. Greisen, K. Cosmic Ray Showers. *Annu. Rev. Nucl. Sci.* **1960**, *10*, 63–108. [CrossRef]
15. Nelson, W.R.; Hirayama, H.; Rogers, D.W. *EGS4 Code System, Report SLAC 265*; Stanford Linear Accelerator Center: Menlo Park, CA, USA, 1985.
16. Grieder, P.K. *Cosmic Rays at Earth*; Elsevier: Amsterdam, The Netherlands, 2001; Chapter 5.4.7, pp. 806–837.
17. Group, P.D.; Zyla, P.; Barnett, R.; Beringer, J.; Dahl, O.; Dwyer, D.; Groom, D.; Lin, C.J.; Lugovsky, K.; Pianori, E.; et al. Review of particle physics. *Prog. Theor. Exp. Phys.* **2020**, *2020*, 083C01. [CrossRef]
18. Matthews, J.; Collaboration, U.M.C. Recent results from the CASA-MIA experiment. *AIP Conf. Proc.* **1995**, *338*, 823–827.
19. Aartsen, M.; Abbasi, R.; Abdou, Y.; Ackermann, M.; Adams, J.; Aguilar, J.; Ahlers, M.; Altmann, D.; Auffenberg, J.; Bai, X.; et al. Measurement of the cosmic ray energy spectrum with IceTop-73. *Phys. Rev. D* **2013**, *88*, 042004. [CrossRef]
20. Axani, S.; Frankiewicz, K.; Conrad, J. CosmicWatch: The Desktop Muon Detector. *J. Instrum.* **2018**, *13*, 03. [CrossRef]
21. Karbowiak, M.; Wibig, T.; Alvarez-Castillo, D.; Beznosko, D.; Duffy, A.R.; Góra, D.; Homola, P.; Kasztelan, M.; Niedźwiecki, M. The first CREDO registration of extensive air shower. *Phys. Educ.* **2020**, *55*, 055021. [CrossRef]
22. Erlykin, A.; Wolfendale, A. Structure in the cosmic ray spectrum: An update. *J. Phys. G Nucl. Part. Phys.* **2001**, *27*, 1005. [CrossRef]
23. Erlykin, A.; Wolfendale, A. Further evidence favouring the single source model for cosmic rays. *Astropart. Phys.* **2005**, *23*, 1–9. [CrossRef]

24. Catanese, M.; Borione, A.; Covault, C.; Cronin, J.; Fick, B.; Fortson, L.; Gibbs, K.; Glasmacher, M.; Green, K.; Kieda, D.; et al. A Search for Ultrahigh-Energy Gamma Rays from EGRET-detected Active Galactic Nuclei Using CASA-MIA. *Astrophys. J.* **1996**, *469*, 572. [CrossRef]
25. Apel, E.W.; Arteaga, J.; Badea, A.; Bekk, K.; Bertaina, M.; Blümer, J.; Bozdog, H.; Brancus, I.; Buchholz, P.; Cantoni, E.; et al. The KASCADE-grande experiment. *Nucl. Instrum. Methods Phys. Res. Sect. A Accel. Spectrometers Detect. Assoc. Equip.* **2010**, *620*, 202–216. [CrossRef]